Interference-Term Elimination for Wigner Distribution Using a Frequency Domain Adaptive Filter*

Shunsuke ISHIMITSU** and Hajime KITAGAWA***

In a nonstationary signal analysis, it has been clarified that the discrete Wigner distribution, WD, is the most suitable distribution. The use of the WD is, however, often complicated by the occurrence of interference terms. Thus, we proposed a modified WD, called the RID (reduced interference distribution), and verified that the RID could markedly suppress the occurrence of interference terms in both the auto- and the cross-WD. In this study, we developed another method which makes use of a block adaptive filter to eliminate interference terms and evaluate them quantitatively. In this method, the least mean square, LMS, algorithm is applied in the frequency domain. Simulated signals of a chirp type and an acoustic signal of a concert hall are analyzed using spectrograms, WD, RID and the new method. From comparisons among the results, it is concluded that the best result can be obtained using the new method proposed in this study.

Key Words: Information Processing and Signal Analysis, Adaptive Control, Computer-Aided Analysis, Sound, Wigner Distribution, Interference-Term Elimination, LMS Algorithm, Block Adaptive Filter, Reduced Interference Distribution, Wavelet Transform

1. Introduction

Spectrum analysis by means of the Fourier transform has been widely used to extract the characteristics of a signal. However its application is confined to either periodic or stationary signals. Nonstationary signals, such as acoustic signals, must be represented in the time-frequency two-dimensional plane, because their frequencies change with time.

Representative methods of time-frequency analysis are those which utilize the Wigner distribution (WD), and spectrogram. A unified framework for these methods was presented by Cohen[1]. In Ref.(1), they are related to each other by smoothing the WD.

Among the methods, the WD is frequently used for nonstationary signal analysis because it provides the highest resolution in both time and frequency domains. Application of the WD, however, is often complicated by the occurrence of interference terms which have no physical meaning[2]. Therefore, to extract reliable information from a signal, those spurious terms must be eliminated. The characteristics of interference terms were elucidated and effective measures were taken to exclude the terms by us[3]. In Ref.(3), a modified WD, called the RID (reduced interference distribution), was proposed. It has been proved that interference terms are markedly suppressed in analytic results obtained using the RID. However, both time and frequency resolutions of the RID are slightly lower than those of the WD, as its algorithm includes a smoothing process.

In this paper, we propose another method which makes use of the adaptive filter, and compare the calculated results with those obtained using the RID for both simulated and measured signals.

2. Nonstationary Signal Analysis

The analytical methods which are related to this study are briefly described.

* Received 13th November, 1995. Japanese original: Trans. Jpn. Soc. Mech. Eng., Vol. 61, No. 584, C (1995), pp. 1490-1495 (Received 1st June, 1994)

** Kawagoe Plant, Pioneer Electronic Corporation, Nishimachi Yamada, Kawagoe, Saitama 350, Japan

*** Production-Systems Engineering, Toyohashi University of Technology, Hibarigaoka Tempaku-cho, Toyohashi, Aichi 441, Japan

2.1 Short-time Fourier transform

The Fourier transform is defined by

$$F_f(\omega)=\int_{-\infty}^{\infty}f(t)e^{-j\omega t}dt. \quad (1)$$

When the signal, $f(t)$, is nonstationary (that is, the frequency spectrum of $f(t)$ is time-variant), the spectrogram of Eq.(2) is applied for the analysis.

$$P_f(t,\omega)=\lim_{T\to\infty}\left|\int_{-T/2}^{T/2}f(\tau)w(t-\tau)e^{-j\omega\tau}d\tau\right|^2/T \quad (2)$$

(The spectrogram is defined as the square of the STFT.) The window length, τ, directly affects the resolutions of both time and frequency, because in Eq. (2), a signal of length τ is assumed to be quasi-stationary. The closer to stationary a signal is, the larger is the value of τ which can be applied and vice versa. Then, to choose a suitable window length, the characteristics of the signal must be investigated before the spectrogram calculation of Eq.(2)

2.2 WD and RID

WD is calculated as

$$W_f(t,\omega)=\frac{1}{2\pi}\int_{-\infty}^{\infty}f\left(t+\frac{\tau}{2}\right)f^*\left(t-\frac{\tau}{2}\right)e^{-j\omega\tau}d\tau. \quad (3)$$

Interference terms are always introduced by the WD calculation. To analyze a signal accurately, those spurious terms must be removed as effectively as possible.

RID was proposed to attain this purpose and it was shown that the algorithm successively reduces interference terms[3),(4)]. In the RID algorithm, the following four procedures are applied to the WD algorithm:

(1) Selection of the most suitable lag window length,

(2) Revision of the analytic signal calculation,

(3) Introduction of the spectrogram calculation in order to mask outer interference terms,

(4) Application of a smoothing procedure for both time and frequency domains, separately.

While (1) and (2) prevent the WD from generating extra terms, (3) and (4) are means to remove extra terms from the WD. As (3) and (4) are filter-based, some restrictions are imposed on both time and frequency resolutions.

2.3 Wavelet transform (WT)

In WT calculation a basic function $\psi_{b,a}(t)$, called an analyzing wavelet, is used;

$$WT_f(b,a)=\frac{1}{\sqrt{a}}\int_{-\infty}^{\infty}\psi_{b,a}^*\left(\frac{t-b}{a}\right)f(t)dt \quad (4)$$

where "a" and "b" are scale and shift parameters, respectively. The analyzing wavelet is translated, and dilated or contracted, using those parameters. As the function must be localized in both time and frequency, the admissibility condition

$$\int_{-\infty}^{\infty}\frac{|\Psi_{b,a}(\omega)|^2}{|\omega|}d\omega<\infty \quad (5)$$

is satisfied, where $\Psi_{b,a}(\omega)$ is the Fourier transform of the analyzing wavelet $\psi_{b,a}(t)$.

Gabor function[5)] is a typical analyzing wavelet. It is expressed as

$$\psi(t)=\pi^{-\frac{1}{4}}\sqrt{\frac{\omega_p}{\gamma}}e^{-\frac{1}{2}(\frac{\omega_p}{\gamma})^2t^2+j\omega_p t} \quad (6)$$

where ω_p is the central frequency of the distribution, and γ is a parameter which determines the degree of localization in the frequency domain. Although the admissibility condition is not satisfied in the strict sense, the introduction of this analyzing wavelet does not cause problems in practical application if γ is chosen to satisfy $|(N+1)\Psi_{b,a}(0)|^2\ll 1$ (where N is the "scale" sampling number).

As the Gabor function provides not only good localization, but also a similar impulse response to the human auditory system, it is used as the analyzing wavelet in this study.

3. Application of a Frequency Domain Adaptive Filter to Eliminate Interference Terms of the WD

Applying a frequency domain adaptive filter, an interference-term elimination algorithm is developed in this study. The algorithm is explained in this section.

3.1 Least mean square, LMS, algorithm

Error signal, $e(n)$, is the sum of a desired signal, $d(n)$, and an output from an adaptive filter, $w_i(n)$;

$$e(n)=d(n)+\sum_{i=0}^{I-1}w_i(n)x(n-i). \quad (7)$$

Let the measurable cost function J be defined as

$$J=E\{e^2(n)\} \quad (8)$$

where $E\{\ \}$ denotes the expectation operator. From Eq.(8), the mean-square error is estimated.

If a reference function, $x(n)$, is correlative with $d(n)$, the value of J can be reduced by applying Eqs. (7) and (8). The optimum filter coefficient to minimize J can be evaluated from gradient vectors of a negative direction as shown in Fig. 1, because those vectors are perpendicular to the contour lines of J and J increases in that direction. The differentiation of J with respect to a coefficient (that is, the gradient vector) is defined by

$$\frac{\partial J}{\partial W_i}=2E\left\{e(n)\frac{\partial e(n)}{\partial W_i}\right\}. \quad (9)$$

Based on the assumption that W_i is time invariant, the partial differentiation of Eq.(7) with respect to W_i is given by

$$\frac{\partial e(n)}{\partial W_i}=x(n-i). \quad (10)$$

By renewing W_i in the $-\nabla J(n)$ direction, $J(n)$ can be minimized with the fewest possible iterations.

That is,

$$W_i(n+1)=W_i(n)-\mu\nabla J(n)$$
$$=W_i(n)+2\mu E[e(n)x(n-i)] \quad (11)$$

where μ is a coefficient of convergence.

To simplify the calculation of Eq. (11), the expectation, $E[e(n)x(n-1)]$, can be replaced by $e(n)x(n-1)$ in the 'LMS algorithm' and the following equation is obtained[6];

$$W_i(n+1)=W_i(n)+2\mu e(n)x(n-i). \quad (12)$$

As the calculation of expectation is omitted, the gradient vector of the algorithm is equal to an instantaneous value of $\nabla J(n)$ at the time n and the cost function, J, becomes larger than the minimum convergent value, J_{min}, by the amount of residual error. This increment is proportional to μ which can be determined from the average energy of $x(n)$[6].

3.2 Frequency domain adaptive filter

A block diagram of the system is shown in Fig. 2. In order to eliminate the interference term after a calculation of the WD is completed, the LMS algorithm is applied in the frequency domain. Then, the elimination procedure can be applied in the final stage of calculation.

$x(n)$ and $d(n)$ are inputted to the system in the format of an L-point data block of the time series.

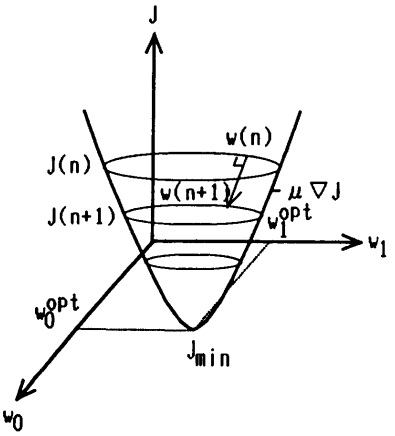

Fig. 1 Steepest-descent algorithm illustrated on a two-dimensional quadratic performance surface

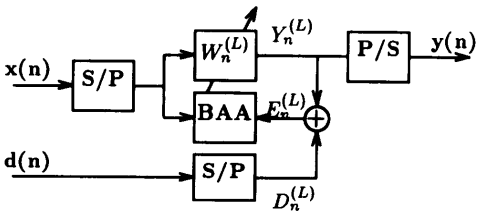

S/P : Serial-to-Parallel Converter
P/S : Parallel-to-Serial Converter
BAA : Block Adaptive Algorithm

Fig. 2 Block diagram of frequency domain adaptive filter

The k-th data block is given by

$$x_k^T=[x(Lk-1)x(Lk-2)\cdots x(Lk-L)] \quad (13)$$

and

$$d_k^T=[d(Lk-1)d(Lk-2)\cdots d(Lk-L)] \quad (14)$$

where $k=1, 2, 3, \cdots$ and T denotes transposition.

The coefficients of both equations, which are complex numbers, are expressed as

$$w_k^T=[w_0(k)w_1(k)\cdots w_{L-1}(k)]. \quad (15)$$

At a discrete frequency $F(f_p)$, where $0\leqq f_p\leqq L-1$, error signals and filter coefficients are given by

$$e_{f_p}(k)=D_{f_p}(k)-w_{f_p}(k)X_{f_p}(k) \quad (16)$$

and

$$w_{f_p}(k+1)=w_{f_p}(k)+2\mu e_{f_p}(k)X_{f_p}^*(k) \quad (17)$$

where "*" denotes the complex conjugate. $D_{f_p}(k)$ and $X_{f_p}(k)$ are pointers of frequency, which represent data locations in digital data processing, of the k-th data block. They are expressed as

$$X_{f_p}(k)=\sum_{l=1}^{L-1}x(Lk-L+l)e^{-j\frac{2\pi f_p l}{L}} \quad (18)$$

and

$$D_{f_p}(k)=\sum_{l=1}^{L-1}d(Lk-L+l)e^{-j\frac{2\pi f_p l}{L}}. \quad (19)$$

3.3 Calculation of the block LMS WD (BLMS-WD)

The algorithm is shown in Fig. 3. The time-frequency distribution obtained by the system is called BLMS-WD. In the analysis, the reference signal, $X(n)$, is inputted to the system in the format of an L-point data block of an original time series. The desired signal, $D(n)$, is converted to an L-point data block and transformed to a time-dependent correlation function. The correlation function is compared with a filtered signal. Then, every data block is transformed to the frequency domain. Any analysis method can be arbitrarily applied to $X(n)$ and $D(n)$. In an analysis in this study, the STFT and the WD are applied to $X(n)$ and $D(n)$, respectively. This is a kind of the BLMS-WD and in this case, the STFT and the WD in each block are simultaneously calculated.

The BLMS-WD offers a very clear understanding of the signal characterization, automatically and systematically. Interference terms of the WD and distributions of the spectrum which may be incoherent with

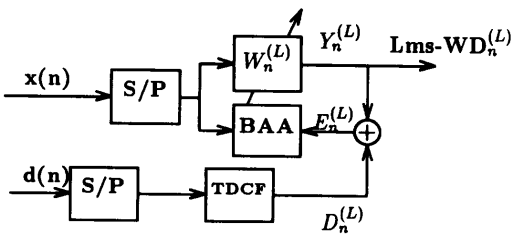

TDCF: Time Dependent Correlation Function

Fig. 3 Block diagram of BLMS-WD

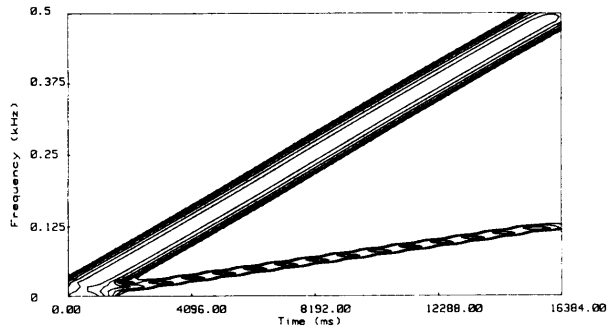

Fig. 4 Spectrogram of chirp signal

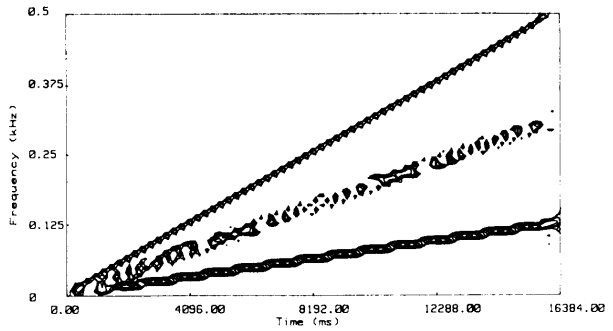

Fig. 5 WD of chirp signal

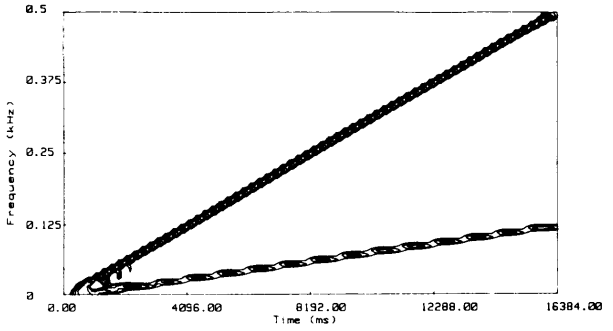

Fig. 6 BLMS-WD of chirp signal

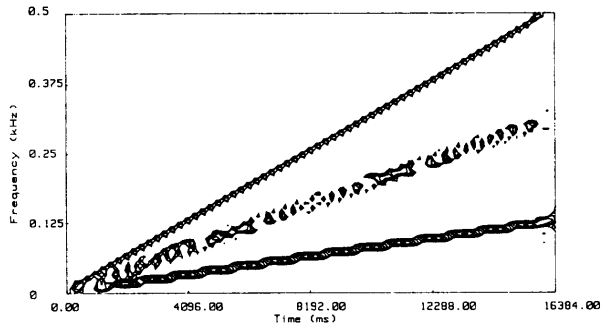

Fig. 7 Error signal of chirp signal in BLMS-WD

the reference signal, are eliminated by the adaptive process. By observing the error signal obtained at the final stage of the process, magnitudes and distributions of the interference terms can be precisely analyzed. In other words, the interference terms in the WD can be quantitatively estimated with ease.

By applying this algorithm, some simulation signals are analyzed. One of them is synthesized from two chirps whose sweeping velocities are 30.5 Hz/s and 7.6 Hz/s. Figure 4 and Fig. 5 show results calculated from the STFT and the WD, respectively. Fig. 6 shows the BLMS-WD with $\mu=0.08$. From Fig. 6, it is proved that the BLMS-WD analysis can eliminate interference terms effectively and provide high resolution. Figure 7 is the error signal of the BLMS-WD. In this figure, a distribution of the outer interference term exists between two signals. In a result obtained using the BLMS-WD, not only the outer interference term but also the inner one can be detected simultaneously as the error signals.

Thus, a 'single process' can be effectively applied to remove both types of interference term in the BLMS-WD calculation, while, in the RID calculation, the STFT is applied to eliminate the outer interference term and a smoothing procedure is used to reduce the inner one. Moreover, in the BLMS-WD algorithm, there is little trade-off between the interference term elimination and the signal resolution, since no smoothing process is used. In the BLMS-WD calculation, it takes 2 sec for the convergence when μ is 0.08. Because the interference term is considered as a noise plant in the adaptive signal processing theory, the filter coefficient is likely to fluctuate even after the convergence. To stabilize this fluctuation sufficiently, a longer convergence time is required. Then, the coefficient of convergence, μ, must be determined by considering the trade-off between the stability and the convergence time of the system. The optimum value of μ depends on the signal characteristics.

4. Analysis of an Acoustic Field

An impulse response of a concert hall is analyzed. The hall is rectangular and is designed to accommodate about 2 000 persons. An impulse is emitted from the center of the stage and it is received at the central seat of the 12th row from the stage.

Results of the analysis are shown in Fig. 8 - Fig. 14. In those figures, sound intensities are divided into 6 levels of -8, -5, -2, 1, 4 and 7 dB.

It is evident from the figures that high-frequency components above 10 kHz attenuate gradually while components below 3.5 kHz remain as the reverberant.

From the results of the STFT, the spectrum distribution may be qualitatively determined, but it is fairly broad because of poor resolution (Fig. 8). For the sake of a quantitative investigation, a region where high energy components are concentrated is analyzed. For example, the area of the address (1.8

kHz, 160 ms) in the time-frequency plane, is a representative region (the region 'A', in Fig. 8). Its acoustic energy is beyond 7 dB and its extent is over 38.4 ms.

In the results of the WD (Fig. 9), the spectrum distribution is fairly sharp but the signal components and the interference terms are not distinguishable. However, judging from the breadth of the distribution, the resolution is improved by about a factor of 3 compared with that of the STFT. In region 'A', both components are not separated and can not be distinguished, but the extent of this region is less than 12.8 ms.

Main components in the reverberant sound are accurately and discretely obtained using the RID. As shown in Fig. 10, the extent of region 'A' is 14 ms and the same resolution of time as that of the WD is maintained.

Since the BLMS-WD shown in Fig. 11 is calculated using a small μ (μ=0.01), the convergence time required is about 100 ms. In this case, the interference-termfree spectra of reverberation are clearly detected. Again, the extent of region 'A' is 12.8 ms and the same resolution of time as that of the WD is completely maintained. As compared with the RID of Fig. 10, the damping characteristic of reverberation obtained from the BLMS-WD is more evident, (Fig. 11), while the RID provides a unclear transition due to smoothing and filtering processes. Thus, it is concluded that the BLMS-WD is a very effective algorithm for accurate analysis of a nonstationary signal.

Next, the same impulse signal is analyzed using the WT (Fig. 12). In the analysis, a Gabor function with ω_p=6.5 kHz, is used as the analyzing wavelet. A multiresolution analysis, which is similar to the human auditory sensation and gives a poorer time resolution in the lower frequency region and a poorer frequency resolution in the higher frequency region, is performed in the calculation of the WT. As 1.8 kHz is a relatively low frequency, the duration of region 'A' is much longer (67.2 ms) than that in other cases. Then, to examine the discontinuity of the impulse more clearly, ω_p is altered to 250 kHz (Fig. 13). As compared with Fig. 12, the regions where the time resolution is improved in Fig. 13, are considered as the

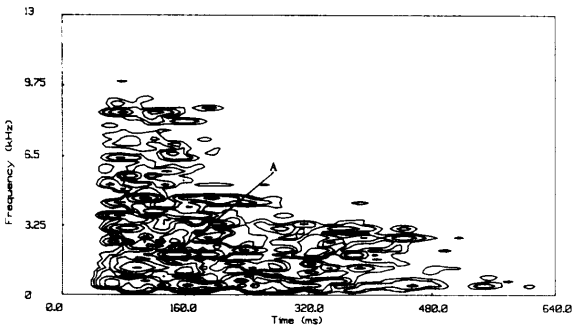

Fig. 8 Spectrogram of a measured signal of a concert hall

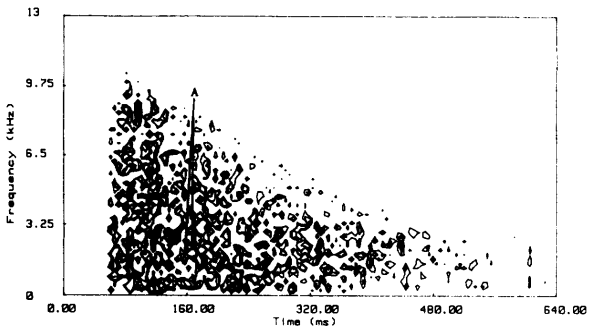

Fig. 9 WD of a measured signal of a concert hall

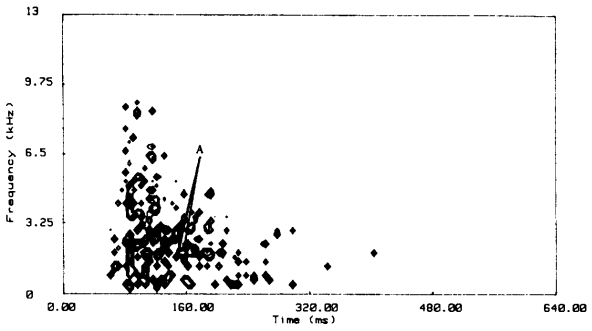

Fig. 10 RID of a measured signal of a concert hall

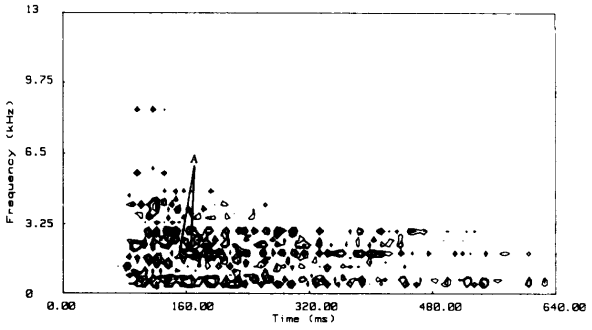

Fig. 11 BLMS-WD of a measured signal of a concert hall

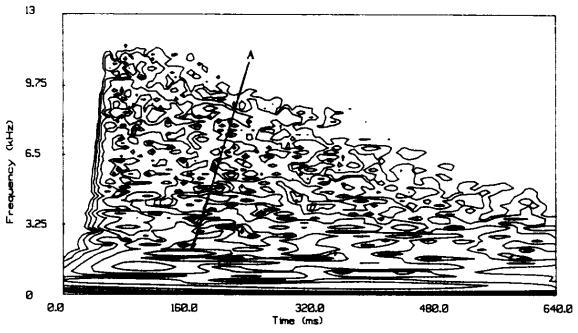

Fig. 12 WT of a measured signal of a concert hall (Central frequency=6.5 kHz)

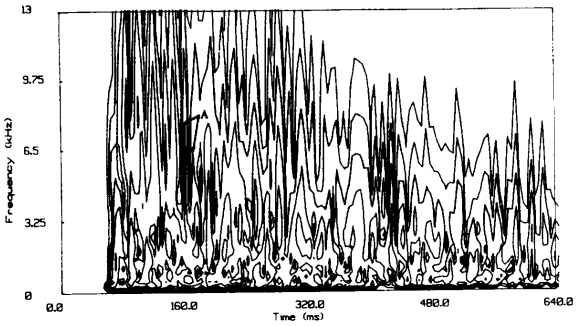

Fig. 13 WT of a measured signal of a concert hall (Central frequency=250 kH)

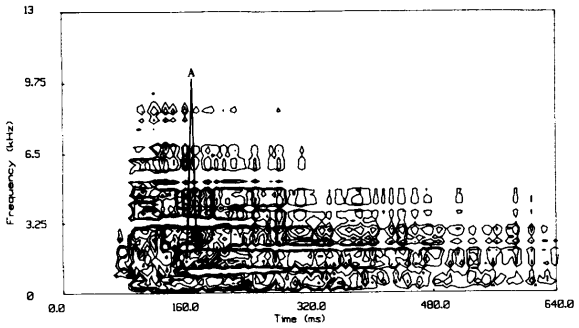

Fig. 14 BLMS-WD of a measured signal of a concert hall, obtained using WT=$x(n)$ and WD=$d(n)$ (Central frequency=250 kH)

discontinuity components. Region 'A' is detected as the components at the peak positions of 160 ms and 171.2 ms on a 1 dB-level contour line. Although the detection of the discontinuity in this manner is possible, the uncertainty of frequency and that of scale become larger, as shown in Fig. 13. Then, it becomes difficult to determine the physical meaning of energy distributions. Region 'A', for example, cannot be identified clearly, because the region is elongated in the frequency direction.

Since any method of two-dimensional analysis can be applied to the BLMS-WD, the WT is applied for $x(n)$ and the WD for $d(n)$ to detect the discontinuity of a signal effectively, or to obtain a characteristic similar to the auditory response. In order to obtain an energy distribution of higher resolution, the BLMS-WD with $\mu=0.01$ is applied for the impulse signal analysis. The result is shown in Fig. 14. The convergence time is 80 ms. The extent of region 'A' is 13 ms and it is approximately equal to that obtained from the WD. Therefore, a more accurate spectrum analysis based on the figure is possible, and accordingly the detection of the discontinuity is feasible, for example, from the concave pattern of the components in a high-frequency region above 8.8 kHz. Namely, a new distribution is obtained from Fig. 14, which makes it possible to detect the discontinuity corresponding to the human auditory sensation, and to analyze the instantaneous energy of a signal, simultaneously. (Alternatively, the WT provides only the discontinuity and the WD, only the instantaneous value of energy).

When a reverberation is supplied by hardware, for example, by a digital signal processor (DSP), the time delay is directly detected by means of reflection signals from the echo. However, the threshold value of time-delay detection is determined without considering the human auditory sensation. By applying the method developed in this study to this field, it is possible to select the most effective time delay and instantaneous energy of an acoustic signal which correspond exactly to the human auditory sensation.

5. Conclusion

An interference-term elimination algorithm using the WD is developed in this study. The algorithm makes use of a frequency domain adaptive filter. It is shown, by the analyses of both simulated and measured signals, that the method makes it possible not only to eliminate both outer and inner interference terms simultaneously, but also to estimate quantitatively the magnitude and the distribution of the terms. The effect of a trade-off between the time-domain and frequency-domain resolutions in this method is less than that in the RID, which is another algorithm for interference-term elimination previously proposed by us. Therefore, it is concluded that a signal can be more precisely represented on the time-frequency plane than other existing methods.

Any time-frequency analysis method can be applied arbitrarily to the desired signal, $d(n)$, or the reference signal, $x(n)$, in the new method. Therefore, by applying several methods to the inputs, simulation signals and a measured impulse signal of a concert hall are analyzed. The results show that such significant characteristics of a signal as the exact instantaneous value of auditory sensation, the discontinuity corresponding to the human auditory sensation and the quantitative estimation of instantaneous energy, are obtained simultaneously. The new method proposed in this study is applicable in various fields of the nonstationary signal analysis.

Thanks are expressed to Mr. S. Mori and Mr. M. Kato at Pioneer Electronic Corporation for their helpful advice.

References

(1) Cohen, L., Time-Frequency Distributions—A Review, Proc. IEEE, Vol. 77, No. 7 (1989), p. 941.
(2) Hlawatsch, F., Interference Terms in the Wigner

Distribution, Proc. Dig. Sig. Proc., Florence, Italy (1984), p. 363.

(3) Ishimitsu, S. and Kitagawa, H., A Revised Discrete Pseudo-Wigner Distribution and its Application to Nonstationary Signal Analyses, Trans. Jpn. Soc. Mech. Eng., (in Japanese), Vol. 57, No. 535, C (1991), p. 141.

(4) Ishimitsu, S., Analysis of the Nonstationary Signals by Means of a Time-Frequency Distribution, Pioneer Tech. Rep., (in Japanese) No. 6 (1992), p. 18.

(5) For example, Meyer, Y., Wavelets, Algorithm and Application, Society for Industrial and Applied Mathematics, (1993), p. 63.

(6) Widrow, B. and Stearns, S.D., Adaptive Signal Processing, (1985), p. 103, Prentice-Hall.